African Journal of Biotechnology Vol. 11(39), pp. 9399-9406, 15 May, 2012
Available online at http://www.academicjournals.org/AJB
DOI: 10.5897/AJB11.3102
ISSN 1684–5315 © 2012 Academic Journals

Full Length Research Paper

The bioaccumulation and toxicity induced by gold nanoparticles in rats *in vivo* can be detected by ultraviolet-visible (UV-visible) spectroscopy

Mohamed Anwar K. Abdelhalim

Department of Physics and Astronomy, College of Science, King Saud University, P.O. Box 2455, Riyadh 11451, Saudi Arabia. E-mail: abdelhalimmak@yahoo.com, mabdulhleem@ksu.edu.sa.

Accepted 4 April, 2012

It is essential to characterize the bioaccumulation and toxicity of gold nanoparticles (GNPs) in blood prior to using them in drug delivery, diagnostics, and treatment. The aim of the present study was to evaluate the blood absorbance spectra after intraperitoneal administration of 50 µl of 10, 20, and 50 nm GNPs in rat for periods of 3 and 7 days to assess their bioaccumulation and toxic effects. Healthy, male Wistar-Kyoto rats, 8 to 12 weeks old (approximately 250 g body weight) were used. 40 rats were divided into four groups; a control group and three test groups (each group was composed of 10 rats); control group (NG: n = 10), test group 1 (G1) (A: infusion of 20 nm GNPs for 3 days; n = 5; B: infusion of 20 nm GNPs for 7 days; n = 5), test group 2 (G2) (A: infusion of 10 nm GNPs for 3 days; n = 5; B: infusion of 10 nm GNPs for 7 days; n = 5) and test group 3 (G3) (A: infusion of 50 nm GNPs for 3 days; n = 5; B: infusion of 50 nm GNPs for 7 days; n = 5). Doses consisting of 50 µl of 10, 20, and 50 nm GNPs dissolved in aqueous solution were administered to the animals via intraperitoneal administration every day for 3 and 7 days. The blood absorbance spectra were obtained using an ultraviolet-visible (UV-VIS) double beam spectrophotometer. Five peaks were observed for normal blood, characteristic of hemoglobin (Hb) macromolecules. After administration of GNPs, absorbance peaks for G1A and G1B decreased significantly and shifted towards the UV compared with the control. The G1A peak decreased significantly compared to G1B. The G2A and G2B peaks also shifted towards the UV compared with the control. All peaks for G2A increased with no significant changes compared with the control while those for G2B decreased significantly. We observed a marked decrease in absorbance for all G3A and G3B peaks and a shifting towards the UV compared with the control. The absorbance peaks for G3A decreased significantly compared with G3B. This study suggests that the decrease in absorbance observed in G1A, G1B, G2A, G3A, and G3B might be attributed to changes in aliphatic and aromatic amino acids, globin-heme, and heme-heme interaction bands. This study demonstrates that as GNP size increases (for example, a decrease in number of GNPs), the absorbance peaks decreased in intensity and shifted towards the UV. The smaller (10 and 20 nm) GNPs demonstrated a smaller decrease in blood absorbance while the larger (50 nm) GNPs indicated a larger decrease in absorbance spectra relative to control. This study also implies that the blood absorbance spectra are particle size and exposure duration dependent, and that UV-visible spectroscopy may be used as a diagnostic for bioaccumulation and toxicity of GNPs in blood. Our results further suggest that the smaller decrease in blood absorbance spectra might indicate that smaller GNPs are mostly taken up and accumulate in tissues, suggesting toxic effects may be induced by smaller GNPs. These conclusions are further supported by histological observations that suggest toxic effects are induced by smaller GNPs deposited in tissue.

Key words: Gold nanoparticles, size, ultraviolet-visible (UV-visible), blood, rats, spectroscopy, toxicity, histology, liver.

INTRODUCTION

The use of gold nanoparticles (GNPs) for detecting and treating cancer is a new and exciting field of research. Current methods of cancer diagnosis and treatment are costly and can be harmful to the body. GNPs, however, offer an inexpensive route to targeting cancerous cells (Caruthers et al., 2007).

GNPs are particularly promising since they are relatively easy to produce in various shapes and can be conjugated with peptides/proteins for targeting to specific molecules (Liu, 2006). In addition, GNPs undergo plasmon resonance when excited by light (Pellequer and Lamprecht, 2009), whereby the gold electrons resonate in response to incoming radiation, causing them to both absorb and scatter light. This effect can be harnessed to either destroy tissue by local heating or to release molecules of therapeutic importance.

The small size of GNPs implies that they could get close to a biological target of interest. Metallic GNPs can resonate in response to a time-varying magnetic field, which has certain advantages related to particle energy transfer (Pellequer and Lamprecht, 2009; Garg et al., 2008; McNeil, 2005; Rosi and Mirkin, 2005; Shrestha et al., 2006). The particle size-dependent distribution of GNPs by organ has been studied *in vivo* (Kamat, 2002; Shipway et al., 2000; Kuwahara et al., 2001; Mirkin et al., 1996; Huber et al., 2004). Orally administrated GNPs appeared in various tissues in mice and the absorbance and distribution was inversely correlated with particle size (Kamat, 2002). The small size of GNPs results in physical and chemical properties that are very different from those of the same material in the bulk form. These properties include a large surface to volume ratio, enhanced or hindered particle aggregation depending on the type of surface modification, enhanced photoemission, high electrical and heat conductivity, and improved surface catalytic activity (Kogan et al., 2007; El-Sayed et al., 2006; Kogan et al., 2006; Zharov et al., 2006; Hirsch et al., 2003).

Ultraviolet-visible (UV–visible) absorbance spectroscopy is widely used for characterizing the optical properties and electronic structure of GNPs because absorbance bands are related to the diameter and aspect ratio of NP metals. Solutions of colloidal GNPs have a distinctive red color, which arises from their tiny dimensions. At nanometer dimensions, the electron cloud can oscillate on the particle surface and absorb electromagnetic radiation at a particular energy. The changes in the UV–visible spectra of the resultant colloids can be measured to study the size effect of metal NPs on the surface plasmon resonance. GNPs exhibit a strong surface plasmon band (SBP), which has been widely investigated (Shim and Gupta, 2007).

There is little *in vivo* data available regarding absorbance spectra as a diagnostic tool for bioaccumulation of GNPs in blood or tissue. To explore the potential role of GNPs in therapeutic and diagnostic applications, we evaluated the absorbance of different GNPs following intraperitoneal administration in rat for 3 and 7 days. We also examined tissue toxicity of smaller GNPs by histological methods.

MATERIALS AND METHODS

GNP size

GNPs of different sizes (10, 20, and 50 nm; MKN-Au-010, MKN-Au-020 and MKN-Au-050, respectively), at a concentration of 0.01%, were purchased from Supplier X. The mean size and morphology of GNPs were evaluated using transmission electron microscopy (TEM).

Animals

Healthy, male Wistar-Kyoto rats were obtained from the Laboratory Animal Center (College of Pharmacy, King Saud University). Rats were 8 to 12 weeks old (approximately 250 g body weight) and were housed in pairs in humidity and temperature-controlled ventilated cages on a 12 h day/night cycle. 40 rats were divided into a control group (NG: n = 10), group 1 (G1) (A: infusion of 20 nm GNPs for 3 days; n = 5; B: 20 nm GNPs for 7 days; n = 5), group 2 (G2) (A: 10 nm GNPs for 3 days; n = 5; B: 10 nm GNPs for 7 days; n = 5) and group 3 (G3) (A: 50 nm GNPs for 3 days; n = 5; B: 50 nm GNPs for 7 days; n = 5). Doses were 50 μl of 10, 20 and 50 nm GNPs dissolved in aqueous solution, and were administered via intraperitoneal administration every day for 3 and 7 days. The rats were anesthetized by inhalation of 5% isoflurane until they exhibited relaxed muscular tonus. Blood samples (~1 ml) was obtained from each rat and added to 0.8 ml of heparin to prevent blood coagulation. Liver tissue was collected from each rat. All experiments were conducted in accordance with the guidelines approved by the King Saud University Local Animal Care and Use Committee.

UV-visible spectroscopy

Absorbance spectrum measurement

Rat blood absorbance infused with 10, 20 and 50 nm GNPs for 3 and 7 days was measured using a UV-VIS double beam spectrophotometer (UV-1601 PC, Shimadzu, Japan; H14 grating UV) through shortwave NIR with optical resolution of 0.4 nm. Absorbance measurements were obtained over 200 to 800 nm at room temperature using quartz cuvettes (1 cm path length). The cuvettes were cleaned before each use by sonicating for 5 min in deionized water followed by rinsing with deionized water. The pH for different GNP samples was kept constant during the measurements.

Histopathological examination

Animals were weighted and examined daily for health and behavioral changes following GNP administration. To evaluate morphological changes, lateral lobe samples from liver were cut rapidly, fixed in neutral buffered formalin (10%), and dehydrated through a series ethanol grades (70, 80, 90, 95 and 100%).

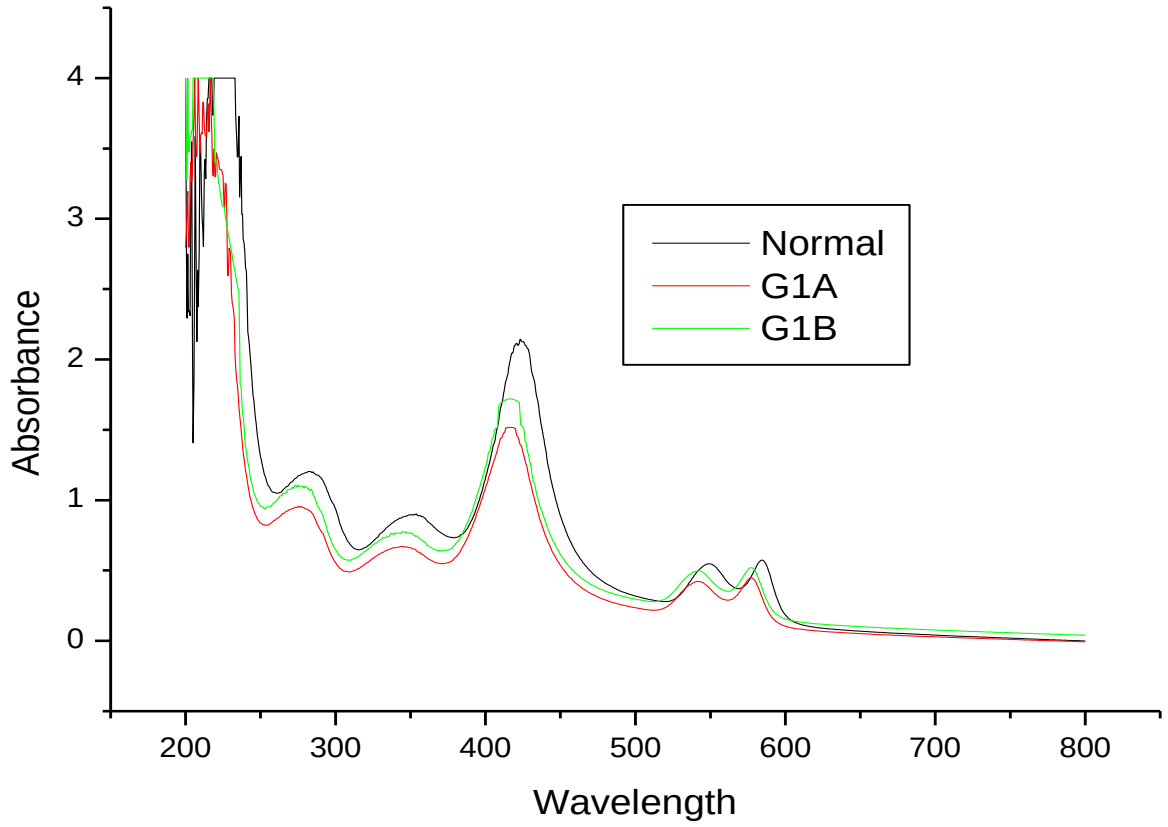

Figure 1. UV-visible absorbance spectra after intraperitoneal administration of 20 nm GNPs for 3 and 7 days.

Samples were then cleared in 2 changes of xylene, impregnated with 2 changes of molten paraffin wax, embedded and blocked. Paraffin sections (4 to 5 µm) were stained with hematoxylin and eosin according to Pearse (1985). Stained sections were examined for hepatocytes and cloudy swelling (ballooning degeneration).

Statistical analysis

To assess the significance of differences between control and the 6 test groups (G1: 20 nm; G2: 10 nm; G3: 50 nm; A: infusion of 50 µl GNPs for 3 days; B: infusion of 50 µl GNPs for 7 days), statistical analysis was performed using one-way analysis of variance (ANOVA) for repeated measurements. Significance was assessed at a 5% confidence level.

RESULTS AND DISCUSSION

Size and morphology of GNPs

The 10 and 20 nm GNPs appeared to have a spherical morphology, whereas the 50 nm GNPs exhibited a hexagonal morphology. The 10, 20, and 50 nm GNPs demonstrate good particle size distribution. The mean size for these GNPs was calculated from the images taken by the transmission electron microscope (TEM). The mean size for 10 nm GNPs was 9.45±1.33 nm, for 20 nm GNPs it was 20.18±1.80 nm, and for 50 nm GNPs, it was 50.73±3.58 nm.

UV-visible spectroscopy

Five hemoglobin (Hb) peaks are characteristic of normal blood (Figure 1). The peak at 280 nm corresponded to the aromatic amino acids, the peak at 340 nm corresponded to globin-heme interaction, the peak at 420 nm corresponded to the heme, the peak at 540 nm corresponded to heme-heme interactions, and the peak at 578 nm corresponded to hemoglobin oxygen affinity (Dacie and Lewis, 1991; Khalifa, 1992).

Following GNP administration, the G1A and G1B peaks decreased significantly and shifted towards the UV, compared with the control. The decrease in absorbance may be attributed to changes in Hb. The absorbance for G1A decreased significantly compared with G1B (Figure 1). The 20 nm GNP absorbance spectra appeared to be exposure duration dependent (Figure 1).

The conformational substrates of Hb appeared normal, indicating stabilization of the conformational substrates. Any change in the Hb absorbance characteristics reflects changes in the heme iron spin state. The spin state absorbance band gives a clear indication regarding

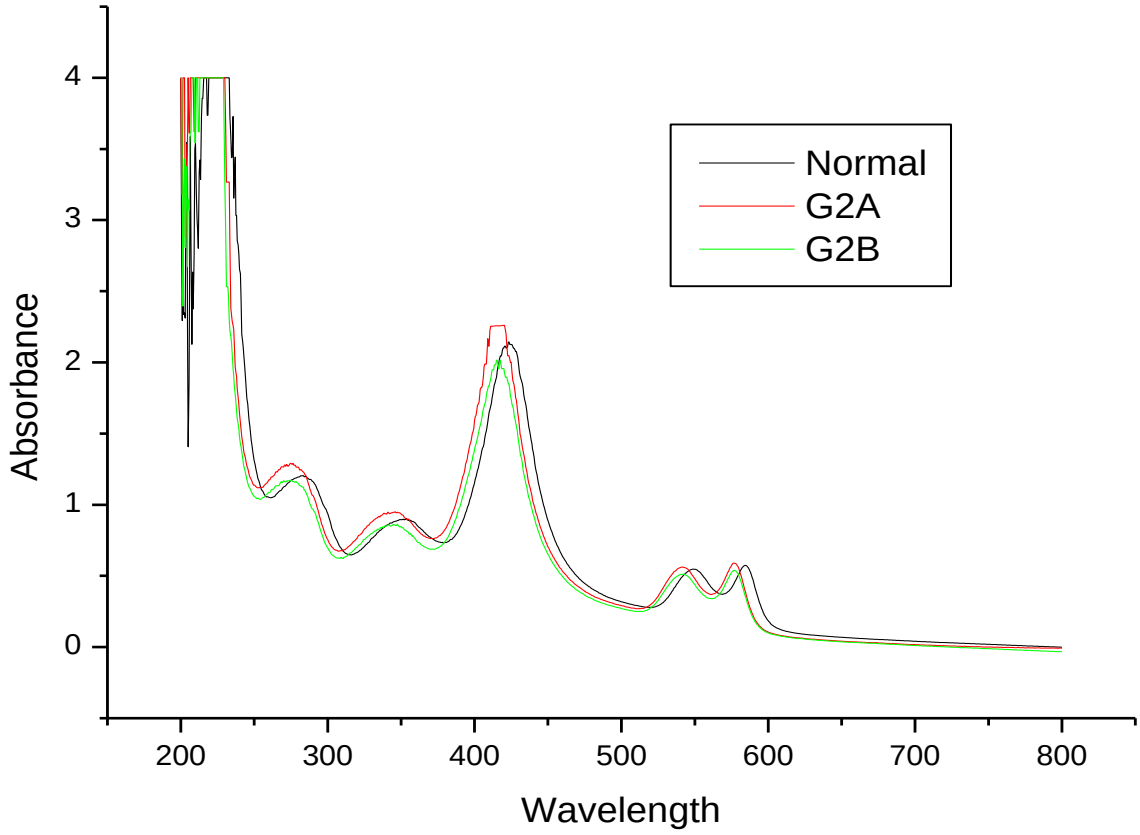

Figure 2. UV-visible absorbance spectra after intraperitoneal administration of 10 nm GNPs for 3 and 7 days.

heme-heme interactions and its affinity for O_2, and consequently, its delivery to tissue (Dacie and Lewis, 1991; Khalifa, 1992).

The absorbance for G2A and G2B underwent a UV-shift compared with the control (Figure 2). All G2A peaks increase in absorbance, with no significant changes compared to control, while the G2B peaks decreased significantly. The 10 nm GNP absorbance spectra are exposure duration dependent (Figure 2).

Proteins are dynamic and motion is essential to their function. A decrease in the absorbance at 280 nm is an indication of abnormal motion, and reflects a deviation from normal structure and function. The extent of deviation reflects the degree of globin unfolding and random motion of the Hb molecule under different levels of oxidative stress (Jetsrisuparb et al., 2006). Elevation in the half Soret band width and the shift towards shorter wavelengths indicate the stretching of iron and nitrogen bonds in the prophyrin ring and an imbalance between protein and heme in the Hb molecule (Khalifa, 1992).

The G3A and G3B spectra show a marked decrease in absorbance for all peaks and a UV shift compared with the control (Figure 3). The absorbance peaks for G3A decreased significantly compared with G3B. This result suggests that the decreased absorbance is particle size dependent and associated with low exposure to GNPs.

Previous studies indicated that increased uptake of GNPs into certain tissues may interfere with the critical biological functions. The exocytosis rate of GNPs was size dependent, with more cellular accumulation of larger GNPs (Kogan et al., 2006). Figure 4 shows that the primary peaks for G1A, G2A and G3A shifted towards the UV compared with the control. G1A and G3A absorbance decreased compared with the control, while G2A absorbance increased. G1B, G2B, and G3B absorbance decreased and underwent a UV shift compared to the control (Figure 5). These results demonstrate that as GNP size increases, that is, when there was decease in the number of NPs, the blood absorbance decreases and shifted towards the UV. In addition, absorbance is particle size and exposure duration dependent.

GNPs absorbed within the systemic circulation can be excreted through various routes. One possible elimination route for GNPs could be renal and biliary clearance. Renal clearance of solid nano-sized materials was affected by particle size and surface charge (Ramanujam et al., 1999; Liu et al., 2007). GNPs for therapeutic applications need to have a long retention time for targeting and therapy. However, a long retention time can evoke toxic effects *in vivo*. Thus, the clearance rate and route of nanomaterials is an important issue (Ramanujam et al., 1999; Kehoe et al., 1988).

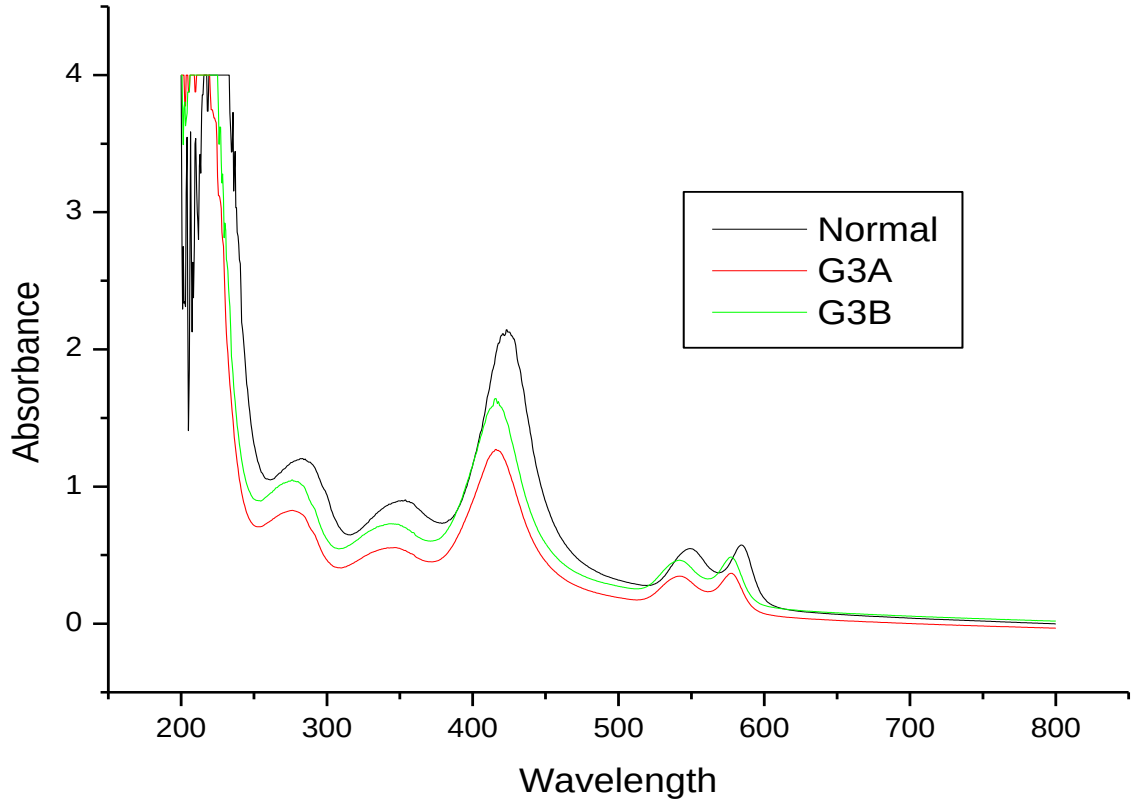

Figure 3. UV-visible absorbance spectra after intraperitoneal administration of 50 nm GNPs for 3 and 7 days.

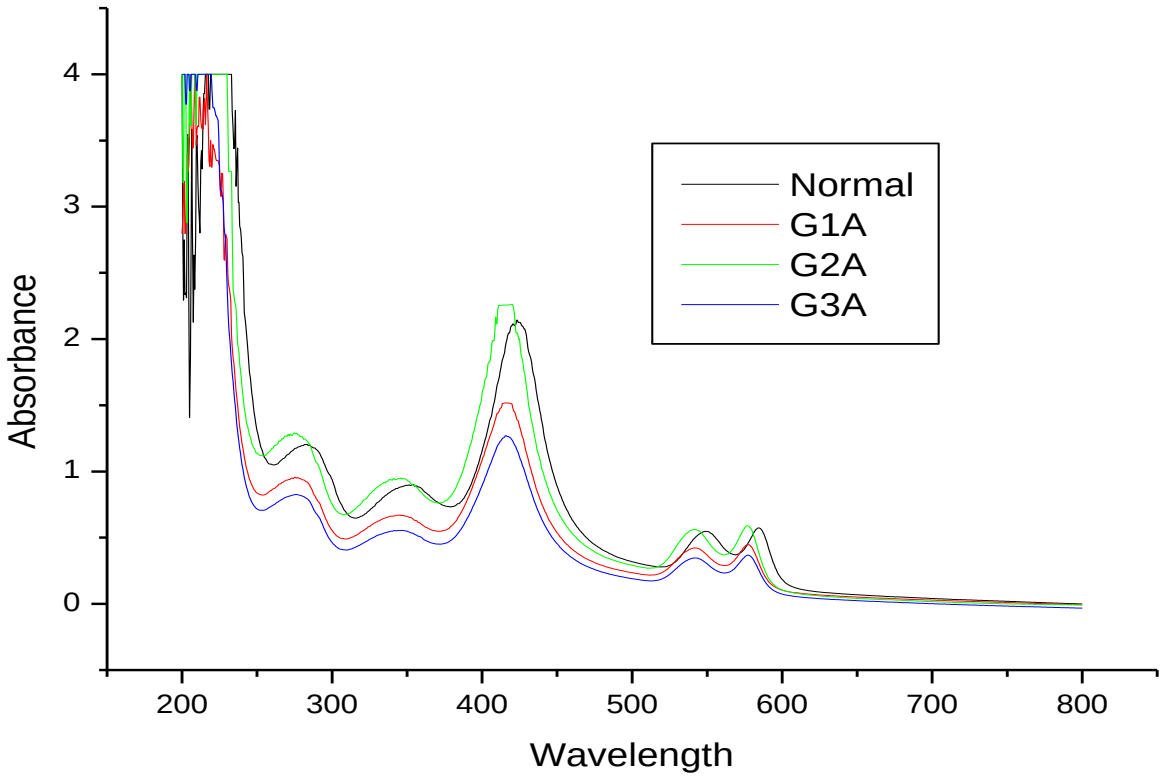

Figure 4. UV-Visible absorbance spectra after administration of 10, 20, and 50 nm GNPs for 3 days.

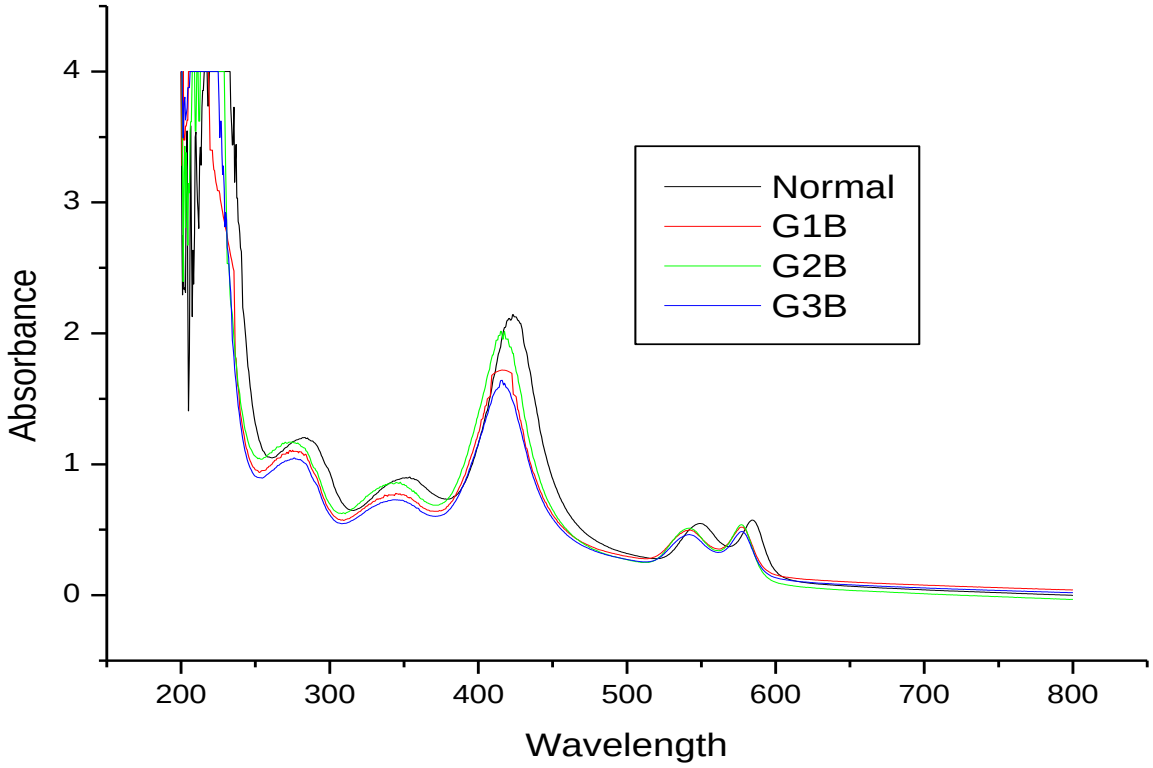

Figure 5. UV-Visible absorbance spectra after the intraperitoneal administration of 10, 20 and 50 nm GNPs for 7 days.

Histological studies

Hepatocytes exhibited cloudy swelling accompanied by leakage of lysosomal hydrolytic enzymes, which resulted in cytoplasmic degeneration and macromolecular crowding, and ballooning degeneration (Figure 6). These changes were more prominent with 10 nm size particles than with larger ones. This may be the result of disturbances in membrane function, leading to water and Na+ influx (Cho et al., 2009; Abdelhalim and Jarrar, 2011; Lasagna-Reeves et al., 2010). Cho et al. (2009) demonstrated that after a single intravenous injection of 13 nm GNPs, gold was found in various organs just 3 and 7 days after injection. However, blood gold levels did not increase in proportion to the dose, indicating that GNPs were taken up and accumulated in tissues.

The accumulation of 12.5 nm GNPs in kidney could be explained by the particle size relative to glomerular pores size, which measures 5.5 nm. This size differential and negative electrostatic potential makes it unlikely that GNPs can pass through the glomerular filtration (Longmire et al., 2008).

In the spleen and liver, the bioaccumulation of GNPs may be regulated by the reticuloendothelial system, which is part of the immune system involved in the uptake and metabolism of exogenous molecules and particles. In addition, GNPs are taken up by kupffer cells in the liver and by macrophages in other tissues (Abdelhalim and Jarrar, 2011), regardless of the particle size (Sadauskas et al., 2007). Abdelhalim and Jarrar, 2011 have reported that the appearance of renal cells cytoplasmic degeneration and nuclear destruction might be an indication of GNPs toxicity.

Conclusion

The aim of the present study was to assess the bioaccumulation and toxicity of GNPs following intraperitoneal administration in rat. Blood absorbance spectra of 10, 20, and 50 nm GNPs at 3 and 7 days were evaluated. Five peaks characterize hemoglobin (Hb) in normal blood. The absorbance for all G1A and G1B peaks decreased significantly and shifted towards the UV compared with the control. The G1A absorbance peaks decreased significantly compared with the G1B peaks.

Our results indicate that as GNP size increases (that is, decease in number of GNPs), absorbance peaks decrease and shifted towards the UV. The data indicates that the smaller (10 and 20 nm) GNPs result in a smaller decrease in absorbance while the larger (50 nm) GNPs result in a larger decrease in absorbance. Absorbance spectra are particle size and exposure duration dependent. In addition, UV-visible absorbance can be used as an important diagnostic tool for GNP bioaccumulation and toxicity in blood.

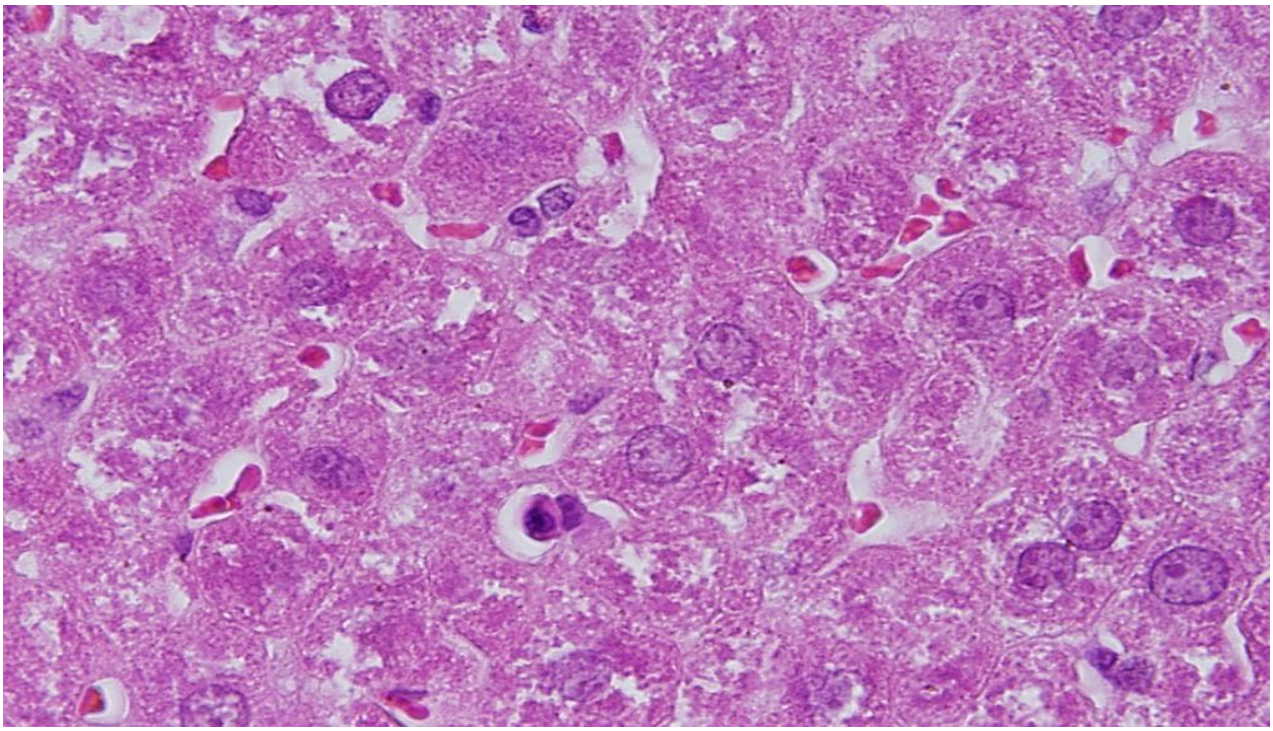

Figure 6. Photomicrograph of hematoxylin and eosin-stained hepatocytes for observing cloudy swelling.

This study suggests that the absorbance decrease observed in all peaks (G1A, G1B, G2A, G3A and G3B) may be attributed to changes in aliphatic and aromatic amino acids, globin-heme and heme-heme interactions. The data also suggests that the less intense absorbance spectra might be indicative of smaller GNPs. Smaller GNPs are more likely to be taken up and accumulate in tissues, resulting in toxic effects. These conclusions were supported by histological investigations that visualized the toxic effects of the smaller GNPs in tissues.

ACKNOWLEDGEMENTS

The author is very grateful to National Plan of Science and Technology NPST. The National Science and Technology Innovation Plan (NSTIP) pro-vided funding for this project through Research No. 08-ADV206-02 and Research No. 09-NAN670-02, College of Science, King Saud University, Saudi Arabia.

REFERENCES

Abdelhalim MAK, Jarrar BM (2011). Gold nanoparticles administration induced prominent inflammatory, central vein intima disruption, fatty change and Kupffer cells hyperplasia. Lipids Health Dis. 10: p. 133.

Abdelhalim MAK, Jarrar BM (2011). The appearance of renal cells cytoplasmic degeneration and nuclear destruction might be an indication of GNPs toxicity. Lipids Health Dis. 10: p. 147.

Caruthers SD, Wickline SA, Lanza GM (2007). Nanotechnological applications in medicine. Curr. Opin. Biotechnol. 18: 26-30.

Cho WS, Cho M, Jeong J, Choi M, Cho HY, Han BS, Kim SH, Kim HO, Lim YT, Chung BH, Jeong J (2009). Acute toxicity and pharmacokinetics of 13 nm-sized PEG-coated gold nanoparticles. Toxicol. Appl. Pharmacol. 236: 16-24.

Dacie JV, Lewis SM (1991). Recognition and measurement of abnormal Hb pigments, In: Churchill L. Practical hematology (7th Ed), Ch 13, UK, p. 190.

El-Sayed IH, Huang X, El-Sayed MA (2006). Selective laser photo-thermal therapy of epithelial carcinoma using anti-EGFR antibody conjugated gold nanoparticles. Cancer Lett. 239:129-135.

Garg J, Poudel B, Chiesa M, Gordon JB, Ma JJ, Wang JB, Ren ZF, Kang YT, Ohtani H, Nanda J, McKinley GH, Chen G (2008). Enhanced thermal conductivity and viscosity of copper nanoparticles in ethylene glycol nanofluid. J Appl Phys 103: 301.

Hirsch LR, Stafford RJ, Bankson JA, Sershen SR, Rivera B, Price RE, Hazle JD, Halas NJ, West JL (2003). Nanoshell-mediated near-infrared thermal therapy of tumors under magnetic resonance guidance. Proc. Natl. Acad. Sci. USA, 100: 13549-13554.

Huber M, Wei TF, Muller UR, Lefebvre PA, Marla SS, Bao YP (2004). Gold nanoparticle probe-based gene expression analysis with unamplified total human RNA. Nucleic Acids Res. 32: e137-e145.

Jetsrisuparb A, Sanchaisuriya k, Fucharoen, Fucharoen S, Wiangnon S, Jetsrisuparb C, Chansoong K (2006). Development ofmsevere anemia during fever episodes in patients with hemoglobin E trait and hemoglobin H disease combinations. J. Pediatric Hematol. Oncol. 28(4): 249-253.

Kamat PV (2002). Photochemical and photocatalytic aspects of metal nanoparticles. J. Phys. Chem. B 106: 7729-7744.

Kehoe DF, Sullivan DM, Smith RL (1988). Determination of gold in animal tissue by graphite furnace atomic absorption spectrophotometry. J. Assoc. Anal. Chem. 71: 1153-1155.

Khalifa AS (1992). Physicochemical structure of Hb in β thalassemia. Egyptian Soc. Hematol. 15: 10-16.

Kogan MJ, Bastus NG, Amigo R, Grillo-Bosch D, Araya E, Turiel A, Labarta A, Giralt E, Puntes VF (2006). Nanoparticle-mediated local and remote manipulation of protein aggregation. Nano. Lett. 6:110-115.

Kogan MJ, Olmedo I, Hosta L, Guerrero AR, Cruz LJ, Albericio F

(2007). Peptides and metallic nanoparticles for biomedical applications. Nanomedicine, 2: 287-306.
Kuwahara Y, Akiyama T, Yamada S (2001). Facile Fabrication of Photoelectrochemical Assemblies Consisting of Gold Nanoparticles and a Tris(2,2'-bipyridine)ruthenium(α)-Viologen Linked Thiol L. Angmuir, 17: 5714-5716.
Lasagna-Reeves C, Gonzalez-Romero D, Barria MA, Olmedo I, Clos A, Ramanujam VMS, Urayama A, Vergara L, Kogan MJ, Soto C (2010). Bioaccumulation and toxicity of gold nanoparticles after repeated administration in mice. Biochem. Biophys. Res. Commun. 393: 649-655
Liu WT (2006). Nanoparticles and their biological and environmental applications. J. Biosci. Bioeng 102: 1-7.
Liu X, Atwater M, Wang J, Huo Q (2007). Extinction coefficient of gold nanoparticles with different sizes and different capping ligands. Colloids Surf. B Biointerfaces, 58: 3-7.
Longmire M, Choyke PL, Kobayashi H (2008). Clearance properties of nano-sized particles and molecules as imaging agents: considerations and caveats. Nanomedicine, 3: 703-717.
McNeil SE (2005). Nanotechnology for the biologist. J. Leukoc Biol. 78: 585-594.
Mirkin CA, Letsinger RL, Mucic RC, Storhoff JJ (1996). A DNA-Based Method for Rationally Assembling Nanoparticles into Macroscopic Materials. Nature, 380: 607-609.
Pearse AE (1985). Histochemistry. Theoritical and applied. Analytical technology 1985, 4th ed. Vol. 2. Churchill-Livingstone, Edinburgh.
Pellequer Y, Lamprecht A (2009). Nanoscale cancer therapeutics. In: Lamprecht A (Ed.). Nanotherapeutics: Drug delivery concepts in nanoscience Chicago: Pan Stanford Publishing, pp. 93-124.
Ramanujam VM, Yokoi K, Egger NG, Dayal HH, Alcock NW, Sandstead HH (1999). Polyatomics in zinc isotope ratio analysis of plasma samples by inductively coupled plasma-mass spectrometry and applicability of nonextracted samples for zinc kinetics. Biol. Trace Elem. Res. 68:143-158.
Rosi NL, Mirkin CA (2005). Nanostructures in biodiagnostics. Chem. Rev. 105: 1547-1562.
Sadauskas E, Wallin H, Stoltenberg M, Vogel U, Doering p, Larsen A, Danscher G (2007). Kupffer cells are central in the removal of nanoparticles from the organism. Part Fibre. Toxicol. 4:10
Shim JY, Gupta VK (2007). Reversible aggregation of gold nanoparticles induced by pH dependent conformational transitions of a self-assembled polypeptide. J. Colloid Interface Sci. 316: 977-983.
Shipway AN, Eugenii K, Itamar W (2000). Nanoparticle arrays on surfaces for electronic, optical, and sensor applications. Chem. Phys. Chem. 1: 18-52.
Shrestha S, Yeung C, Nunnerley C, Tsang S (2006). Comparison of morphology and electrical conductivity of various thin films containing nano-crystalline praseodymium oxide particles. Sens Actuators A Phys 136: 191-198.
Zharov VP, Mercer KE, Galitovskaya EN, Smeltzer MS (2006). Photothermal nanotherapeutics and nanodiagnostics for selective killing of bacteria targeted with gold nanoparticles. Biophys. J. 90: 619-627.